第 21 卷 第 1 期
2006 年 2 月

实 验 力 学
JOURNAL OF EXPERIMENTAL MECHANICS

Vol. 21 No. 1
Feb. 2006

文章编号:1001-4888(2006)01--

Digital Holography—A New Paradigm In Imaging, Microscopy and Metrology*

Anand Asundi, Vijay Raj Singh, Pinghua Zhong

(School of Mechanical and Aerospace Engineering, Nanyang Technological University, Singapore)

Abstract: Digital Holography (DH) has brought a new impetus to the field of holography. The fields of imaging, microscopy and metrology have all benefited from these developments. In this paper some of these developments will be described with some applications in the fields of color imaging, amplitude and phase microscopy and dynamic metrology. It is envisaged that this field will rapidly advance in the next couple of years and become an expected imaging and measurement modality especially in the field of micro, nano and bio sciences.

Key words: ???

0 Introduction

Amplitude and phase are the two main informations used to characterize any wave. Optical detectors such as photographic films or CCDs record only the intensity, which is the square of the amplitude. Thus the phase information is lost in this process. Holography records both the amplitude and phase of the wave. Dennis Gabor[1,2] developed the theory of holography while working to improve the resolution of the electron microscope. When any object wave interferes with a reference wave, the recorded interference pattern is called hologram. The amplitude and phase information of the object wave is encoded in the interference pattern, and can be played back or reconstructed by illuminating the hologram with the same reference wave as used during recording process. Holography is thus a two-step process and makes use of the wave nature of light to record (interference) and reconstruct (diffraction) the image.

The major drawback of classical holography is use of photographic plates for recording, and the subsequent need for wet chemical development process that is costly and time-consuming. With the growing development of digital computers and Charged Coupled Devices (CCD), digital holography is being explored. There are two types of digital holography - in the first a hologram can be generated in the computer by digital simulating the interference of the object and reference beams. These have been used in the development of Holographic (diffractive) Optical Elements (HOEs). In this case, since the result of the Computer Generated Holograms (CGH) need to be evaluated rapidly, optical reconstruction using Spatial Light Modulators (SLM) have been explored. The second approach is to record an optically generated hologram using a CCD. This digital hologram is then reconstructed

* Received date: 2005-05-23
Corresponding author:

numerically. In this article, Digital Holography refers to the latter.

The limited resolution of the CCD sensors is the main drawback for digital holography. The best commercially available CCD has a resolution of about 150 lines/mm, which compares poorly with the about 5000 lines/mm resolution of conventional holographic films. This limited resolution limits the frequency of the interference pattern that can be recorded and hence restricts the angle between object and reference beams to a few degrees. However, the numerical reconstruction process is very flexible and can be used in a variety of ways to overcome the deficiency of small interference angle. Furthermore, efficient numerical algorithms aided by fast processing speed, allows quantitative evaluation of holographic reconstruction for real time investigations. Indeed Digital Holography enables one to reconstruct the Gabor Hologram in all its splendour. In addition since the object wave is determined it is possible to separate the amplitude and phase information of the object. These features make it as a perfect tool for imaging, microscopy and metrology. In this article following a brief review of Digital Holography, applications to colour and phase imaging, microscopy and dynamic measurement are described.

1 Digital holography

Digital holography is classified as a Fresnel or a Fraunhofer hologram based on the diffraction region of the object wave where the digital holograms are recorded. The setup for Digital Fresnel is shown in Figure 1, wherein the interference pattern of reference and object beams is recorded by CCD placed in the Fresnel diffraction region of the object wave. The collimated reference beam is incident normally to the CCD and θ is the offset angle of the object.

For a digital Fraunhofer hologram, a lens is used to generate a Fraunhofer diffraction pattern of the object wave as shown in Fig. 2.

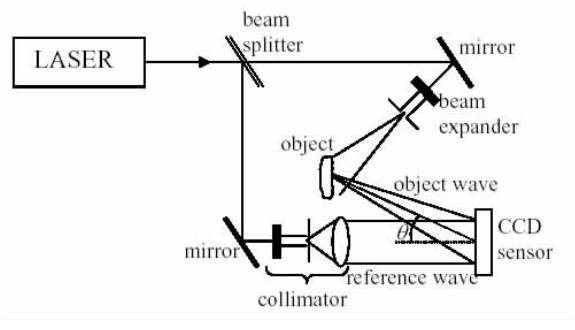

Fig. 1 Fresnel digital holography

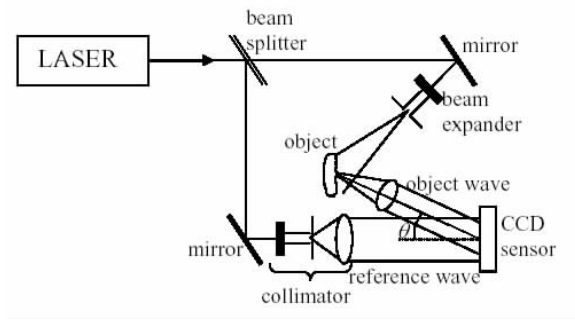

Fig. 2 Fraunhofer digital holography

In 1994, Schnars and Juptner, showed for the first time that the CCD target can directly record off axis Fresnel's holograms and computer can be used for numerical reconstruction process by simulating the Fresnel-Kirchhoff diffraction integral[3].

1.1 Digital recording methods

Let (x, y) be the coordinates in the object plane and (ξ, η) that in the hologram plane. The hologram, which is the interference of the object wave $O(\xi, \eta)$ and reference wave $R(\xi, \eta)$, can be written as

$$H(\xi,\eta) = |O(\xi,\eta)|^2 + |R(\xi,\eta)|^2 + O^*(\xi,\eta)\,R(\xi,\eta) + O(\xi,\eta)\,R^*(\xi,\eta) \tag{1}$$

O^* and R^* is the complex conjugate of the O and R respectively.

The CCD, placed at the hologram plane, records this interference pattern. The recorded pattern

is sampled into a two-dimensional array of discrete numbers. Let the CCD have $M\times N$ pixels of size $\Delta\xi$ and $\Delta\eta$. The digitally sampled holograms $H(m,n)$, can be written as[4]

$$H(m,n)=\left[H(\xi,\eta)^{*}\,rect\left(\frac{\xi}{\alpha\Delta\xi},\frac{\eta}{\beta\Delta\eta}\right)\right]\times rect\left(\frac{\xi}{M\Delta\xi},\frac{\eta}{N\Delta\eta}\right)comb\left(\frac{\xi}{\Delta\xi},\frac{\eta}{\Delta\eta}\right) \tag{2}$$

Where $*$ represents the two-dimensional convolution and $(\alpha,\beta)\in[0,1]$ are the fill factors of the CCD pixels.

The poor resolution of the available CCD sensors imposes strong constraints on the angle between object and reference waves to fulfil the sampling theorem. As long as the sampling theorem is satisfied, the numerically reconstructed image will have no loss of information. The angle between the object and reference waves is dependent on the distance of the object from CCD and the size of the object. Therefore the simplest way to reduce the angle between waves is either by reducing the apparent size of the object or by increasing its distance from CCD. A study of the object size and CCD resolution is given in the reference[5]. For small objects, a microscopic objective is used to magnify the object wave and then interfere with the reference wave[6]. On the other hand for large objects a diverging lens is used to get a demagnified virtual image of the object to reduce the object spatial frequency and the wavefield of the virtual image rather then the object is recorded by the CCD[7].

1.2 Numerical reconstruction methods

Figure 3 shows the coordinate system for recording and reconstruction in digital holography. The interference of object and reference beam is recorded at the hologram plane by the CCD sensor. The recorded hologram $H(\xi,\eta)$ is digitised.

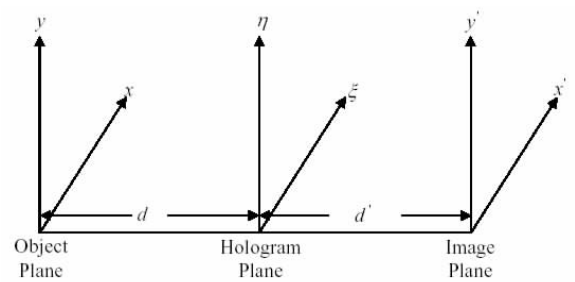

Fig. 3 Coordinate system for digital holography

The reconstruction of hologram is a diffraction process. The hologram $H(\xi,\eta)$ is illuminated by the reconstructed wave $R(\xi,\eta)$ and then the reconstructed wavefield at the image plane (x',y') at distance d' is given by the Fresnel diffraction formula

$$U(x',y')=\frac{e^{ikd'}}{i\lambda d'}\int_{-\infty}^{\infty}\int_{-\infty}^{\infty}H(\xi,\eta)R(\xi,\eta)\exp\left[\frac{i\pi}{\lambda d'}\{(x'-\xi)^2+(y'-\eta)^2\}\right]d\xi d\eta \tag{3}$$

where $k=\dfrac{2\pi}{\lambda}$, is the wave function.

The impulse response $g(\xi,\eta)$ of the coherent optical system can be defined as defined as

$$g(\xi,\eta)=\frac{e^{ikd'}}{i\lambda d'}\exp\left\{\frac{i\pi}{\lambda d'}(\xi^2+\eta^2)\right\} \tag{4}$$

Substituting eqn (4) into eqn (3) gives

$$U(x',y')=e^{i\pi d'(\nu^2+\mu^2)}\int_{-\infty}^{\infty}\int_{-\infty}^{\infty}H(\xi,\eta)R(\xi,\eta)g(\xi,\eta)\exp\left[-2\pi i\{\xi\nu+\eta\mu\}\right]d\xi d\eta \tag{5}$$

Here $\nu=\dfrac{x'}{\lambda d'}$ and $\mu=\dfrac{y'}{\lambda d'}$ are spatial frequencies. The reconstructed object wavefield is simply the Fourier transform of the product of the hologram, reconstruction wave and the impulse response function. i. e.

$$U(x',y')=\mathcal{F}\{H(\xi,\eta)R(\xi,\eta)g(\xi,\eta)\} \tag{6}$$

The pixel size of the numerically reconstructed image by this method varies with the reconstruction distance and is given by

$$\Delta x' = \frac{\lambda d'}{M\Delta\xi}, \quad \Delta y' = \frac{\lambda d'}{N\Delta\eta} \tag{7}$$

When reconstructed wave is the complex conjugate of the reference wave, then real image of the object is formed at the reconstruction distance d same as recording distance the hologram.

The intensity and phase can be written as

$$I(x',y') = |U(x',y')|^2 \tag{8a}$$

$$\varphi(x',y') = \arctan\frac{\mathrm{Im}(U(x',y'))}{\mathrm{Re}(U(x',y'))} \tag{8b}$$

If the pitch of the reconstructed image is to be kept constant irrespective of the reconstruction distance, the convolution approach is used for reconstruction. It can be shown that the diffraction integral, eqn. (3) becomes a convolution for linear space invariant system. The reconstructed object wavefield can then be written as

$$U(x',y') = [H(\xi,\eta)R(\xi,\eta)] \otimes [g(\xi,\eta)] \tag{9a}$$

where $\otimes$ shows the two dimensional convolution. The reconstructed wavefield can be calculated by using the convolution theorem as,

$$U(x',y') = \mathcal{T}^{-1}[\mathcal{T}\{H(\xi,\eta)R(\xi,\eta)\}\mathcal{T}\{g(\xi,\eta)\}] \tag{9b}$$

The pixel size of the reconstructed image is same as the pixel size of the CCD and does not vary with the reconstruction distance i. e. $\Delta x' = \Delta\xi$ and $\Delta y' = \Delta\eta$.

The reconstructed wave field contains mainly three parts, (i) zero order term, (ii) real image wave, and (iii) conjugate image wave (also called twin image). Zero order term or DC term is the un-diffracted wave from the hologram and appears as the bright background in the reconstructed image. This term can be understood from the hologram equation:

$$H(\xi,\eta) = |O(\xi,\eta)|^2 + |R(\xi,\eta)|^2 + O^*(\xi,\eta)R(\xi,\eta) + O(\xi,\eta)R^*(\xi,\eta) \tag{10}$$

In this equation the first two terms $|O(\xi,\eta)|^2 + |R(\xi,\eta)|^2$ constitute the zero order term, O^* is the conjugate image wave and O is the real image wave. For the in-line setup, the appearance zero order term degrades the image quality; hence efforts were made to eliminate it from the reconstructed image.

This can be simply done by separately recording the object wave $|O(\xi,\eta)|^2$ and the reference wave $|R(\xi,\eta)|^2$ and then subtract these from recorded hologram before reconstruction[8]. However, this process is not popular because of the additional measurements required. The zero order term can also be suppressed by numerically subtracting the average intensity of all pixels $H_m(k\Delta\xi, l\Delta\eta)$ from the recorded digital hologram $H(k\Delta\xi, l\Delta\eta)$[9]. Zero order term suppression is also possible by other methods[10−14].

2 Applications

2.1 Amplitude Imaging-Particles analysis

Particles analysis is one of the major applications of holography. Direct recording of holograms by CCD sensors and numerical reconstruction method can be applied for particles analysis[15]. The potential for measurement of the size, location, speed, and three-dimensional spatial distribution of particles make holographic techniques more popular then the existing techniques like laser-doppler-anemometry (LDA), phase-doppler-anemometry (PDA)[16]. The small angle between the object and reference waves results in three problems during the reconstruction process: overlap of the object wave and the un-diffracted zero order wave; overlap of the real and virtual images and finally appearance of the defocused images of object outside the plane of reconstruction. The first two effects

have been resolved using various methods and are usually not a major problem especially if the particles are small. However the third effect has not been addressed and thus the full capability of holography has not been exploited. Various approaches using image processing, curve fitting and thresholding have been proposed to accurately locate a particle along the axial (depth) direction as well as its size measurements[17—19].

A novel method to eliminate the defocused particles and display a slice containing only the in-focus parts of the image is presented here. Furthermore, only a single hologram is necessary and no other curve fitting or processing is required. The bright background is also simultaneously minimised and although the effect of the twin image (not a major problem for small particles) can be reduced as well.

The property that only the in-focus reconstructed image wave is a real quantity is used to minimise the out-of-focus and other terms effects and thus provide an image slice with only the focused parts of the object visible. The depth of focus of the system limits the isolation of the slice. The wavefield is reconstructed by convolution methods and if opaque particles are the object and A_0 represents the their amplitude transmittance, then the subtraction of in-focus $U(x', y', d)$ and out-of focus $U(x', y', d+\Delta d)$ wavefields represent mainly the real part of reconstructed wave, and for amplitude image this difference represents only amplitude of the focused particles (at reconstruction distance d) i. e.

$$U(x', y', d) - U(x', y', d+\Delta d) \approx A_0^* \tag{11}$$

Thus subtraction of the two reconstructed waves eliminates the direct wave and the defocused object waves simultaneously.

To demonstrate this effect the experimental set-up as shown in Figure 4 was used. A laser beam was used to illuminate a 4- mm thick glass slide, which had a few 5～10 μm particles on either face.

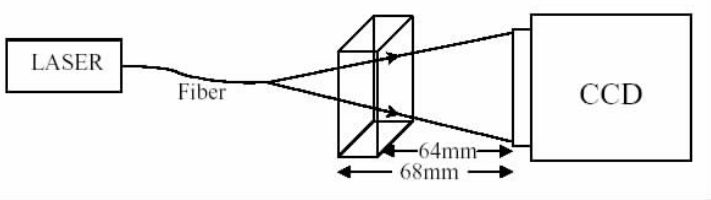

Fig. 4　Experimental set-up for particles analysis

Figure 5 (a) and (b) show the amplitude images at reconstruction distances 64mm and 68mm using the CV method and Figure 5 (c) and (d) shows the corresponding subtracted images for front and backsides of glass plate.

2.2 Phase imaging

Traditional numerical reconstructions can only get the amplitude-contrast images from which only the intensity of the reconstructed wave field is considered. Furthermore, holographic interferometry can only numerically reconstruct the interference phase of two different states of the object. However, these methods mentioned above can not reconstruct a phase-contrast image from a single hologram. Cuche et al[20, 21] proposed a new approach for reconstruction of quantitative phase-contrast image. For phase-contrast imaging, during the numerical reconstruction process, a digital reconstruction wave must be simulated as R_d:

$$R_d(\xi, \eta) = A_R \exp[i \frac{2\pi}{\lambda}(k_x k \Delta\xi + k_y l \Delta\eta)] \tag{12}$$

where k_x and k_y are the two components of the wave vector, A_R is the amplitude of reconstruction wave and generally set to unity ($A_R=1$). Assume R_d is completely a replica of reference wave during

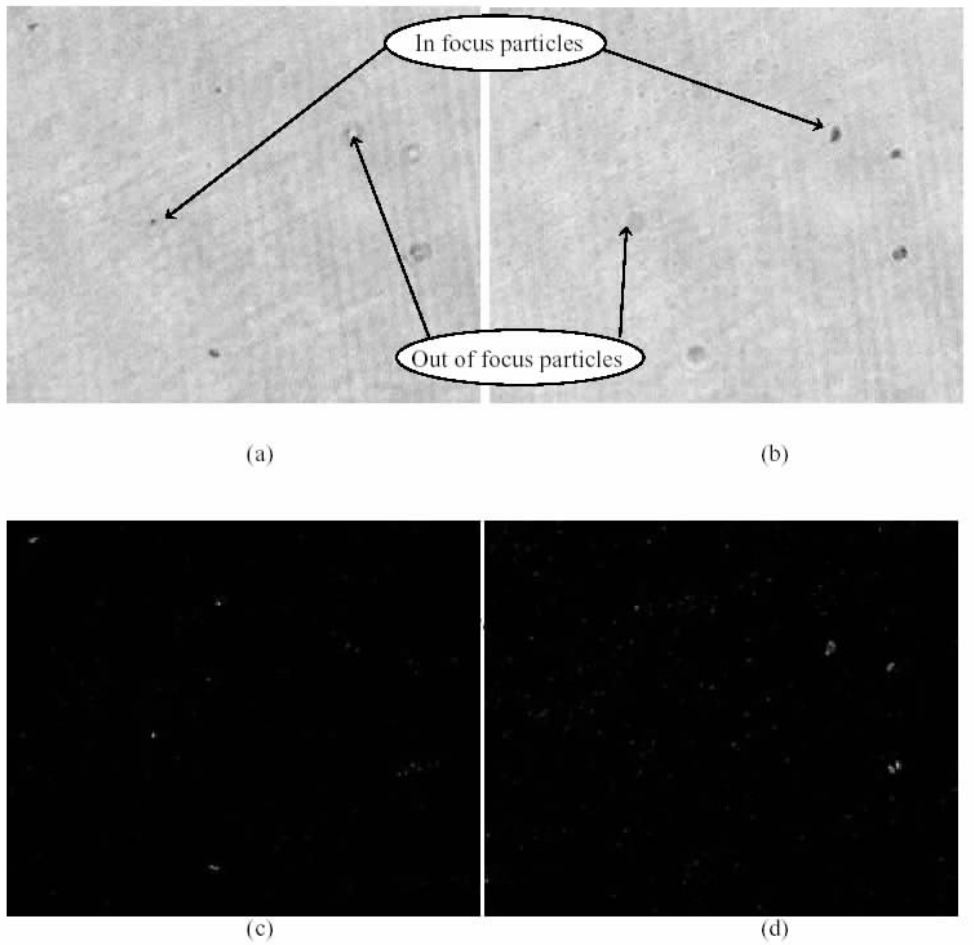

Fig. 5 (a) & (b) Reconstructed amplitudes images of particles, and (c) & (d) corresponding subtracted images

recording process, so k_x and k_y should be adjusted until the propagation direction of R_d matches that of the reference wave as closely as possible. Then the reconstructed wavefield at the image plane (x', y') is given by convolution approach:

$$U(x', y') = \mathcal{T}^{-1}\left[\mathcal{T}\{H(\xi, \eta)R_d(\xi, \eta)\}\mathcal{T}\{g(\xi, \eta)\}\right] \tag{13}$$

As shown in Fig. 6, fine adjustment of k_x and k_y will result in a phase contrast image.

2.3 **Dynamic applications: vibration analysis**

The most remarkable application of holography is the interferometric comparison of diffuse wavefronts. This involves recording digital holograms of the object in two different states. By reconstructing the holograms before and after deformation, the two wavefields can be subtracted to produce a fringe pattern that describes the changes that occurred between the two states of the object. Dynamic behaviour of the objects is studied by pulsed digital holography. Digital holograms are recorded corresponding to each pulse and reconstructed phase subtraction gives the deformation in respective situation[22—24]. The other method for dynamic measurement is the time average recording of vibrating objects wherein the exposure time is longer than the period of vibration. In this case the amplitude distribution of the object is modulated by the zero order Bessel function J_0.

Time average digital holography shows some interesting features not available with standard time average holography. Consider the vibration of a thin circular diaphragm (diameter 12mm) excited at different frequencies and amplitudes. Subtraction of numerically reconstructed wavefields from time average holograms recorded at different amplitudes with same vibration frequency shows the both time

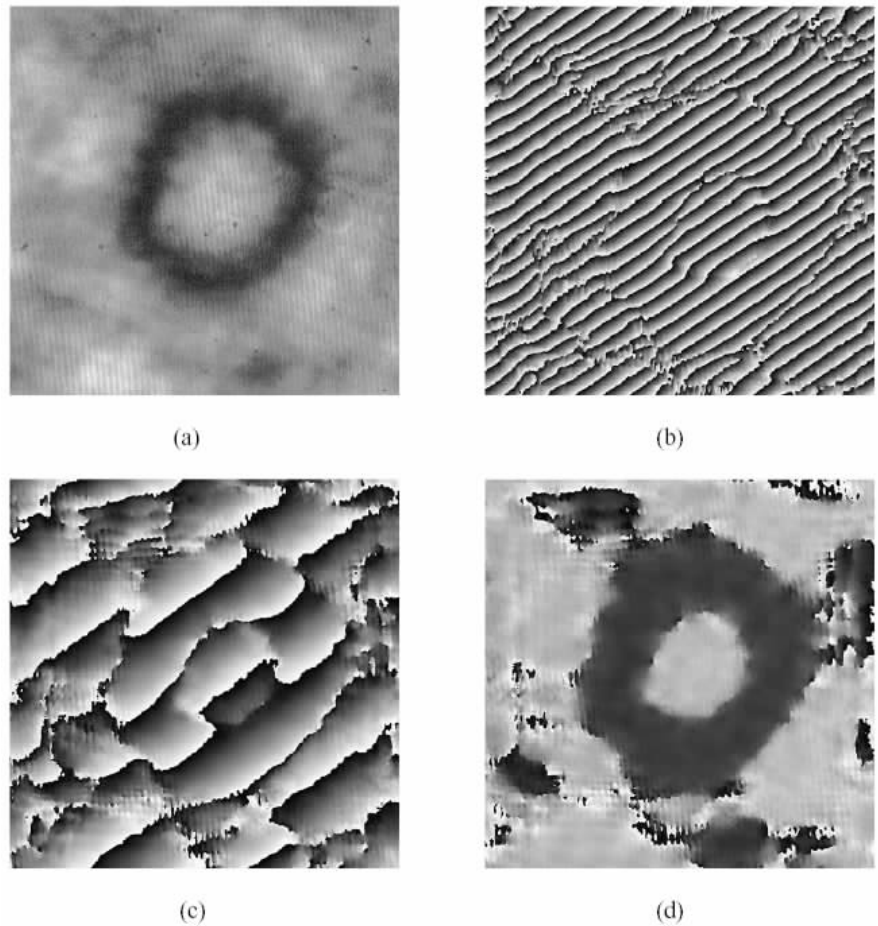

Fig. 6　A single hologram and phase-contrast images reconstructed by different values of k_x and k_y. (a) Hologram of a micro hole, (b) Phase image with $k_x=2\times10^{-3}$ and $k_y=3\times10^{-3}$, (c) Phase image with $k_x=5\times10^{-4}$ and $k_y=7\times10^{-4}$. (d) Phase image with $k_x=5\times10^{-6}$ and $k_y=2\times10^{-3}$

average as well as static deformation fringes. It is possible to separate both the time average and static deformation fringes from each other. This feature is not available with traditional time average holography or speckle methods.

The displacement of an object, sinusoidally vibrating along z-direction placed in (x,y) plane can be written as

$$z(x,y,t) = z(x,y)\cos\omega t \tag{14}$$

where ω is the frequency of vibration. $O(x,y)$ is the object wave scattered from the vibrating object and can be written as

$$O(x,y) = O_0(x,y)\mathrm{e}^{i\phi_0(x,y)}\,\mathrm{e}^{i\frac{4\pi}{\lambda}z(x,y,t)} \tag{15}$$

Here $O_0(x,y)$ is the amplitude, $\phi_0(x,y)$ phase term due to mean static state of vibration of the object. For time average recording the object wave becomes

$$O(x,y,t) = \frac{1}{T}\int_0^T O(x,y,t)dt = O_0\,\mathrm{e}^{i\phi_0(x,y)}J_0\left[\frac{4\pi}{\lambda}z(x,y)\right] \tag{16}$$

where J_0 is the zero-order Bessel function. This object wave interferes with the plane reference wave and is recorded by a CCD at the hologram plane. The numerically reconstructed real image wave is not exactly same as the object wave as defined is equation (16), because it is convolved with the filtering function of the discrete Fresnel transform and becomes spatially enlarged. However the fundamental form of the reconstructed real image wave is same.

If two time average holograms are recorded with different amplitudes at same frequency, then the subtraction of reconstructed real image waves contains both Bessel function as well as phase difference term. The mean static deformation difference due to a change in the amplitude of vibration results in the static deformation fringes along-with the vibration fringes. Thus subtraction of phases gives only the static deformation fringes and vibration fringes can be obtained by intensity subtraction. Figure 7 shows the results of a membrane vibrating at 10.5 kHz. Figure 7(a) is the subtraction of reconstructed wavefiles and shows the combined time average J_0 and the static deformation fringes, Fig. 7(b) shows the result of subtracting of amplitudes and hence only the J_0 fringes are seen and Fig. 7(c) shows the subtraction of the phase from two time average recoding showing the static deformation fringes only.

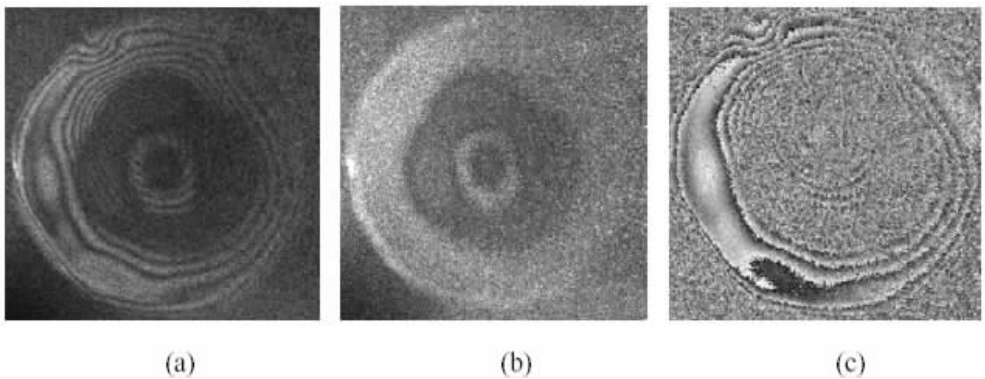

Fig. 7 Reconstruction of two time average digital holograms at a frequency of 10.5 kHz but with different amplitudes (a) Wavefield subtraction, (b) Intensity subtraction, and (c) Phase subtraction

2.4 Colour digital holography

In holography true colour images can be reconstructed from a hologram recorded with three lasers with appropriate red, green and blue wavelength. The availability of colour CCDs makes it possible to record colour digital holograms and thus numerical reconstruct true colour holograms. An experimental set-up for in-line colour digital holography with two wavelengths is shown in Fig. 8. Two fiber coupled lasers - He-Ne (632nm) and frequency doubled Nd-Yag (532nm) are combined with a beam splitter and then collimated. This beam illuminates a coloured photographic negative and the hologram is recorded by a colour CCD with 720×1280 square pixels 6 μm in size.

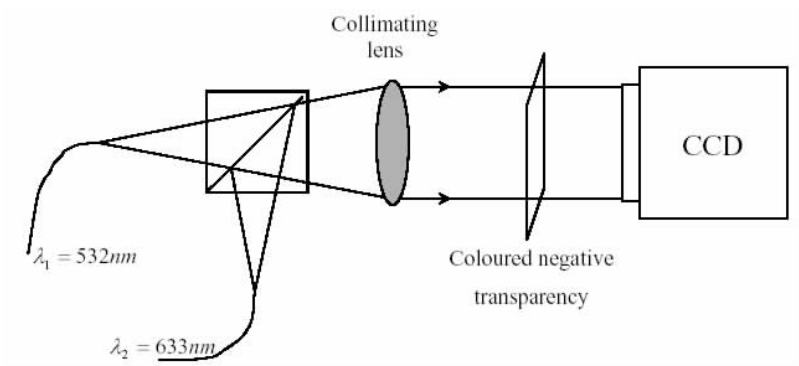

Fig. 8 In-line colour digital holography for transparent objects with two wavelengths

The numerical reconstruction process is performed using the convolution approach because the pixel size of reconstructed image is constant and equal to the size of CCD pixel. The object is shown in Figure 9(a) and the numerically reconstructed image is shown in Figure 9(b).

Fig. 9 (a) Negative transparency, and (b) Numerically reconstructed coloured image

References:

[1] Gabor D. A new microscopic Principle[J]. Nature, 1948,161:777—778.

[2] Gabor D. Microscopy by reconstructed wavefronts[J]. Proc. Royal. Soc., 1949,197:454—487.

[3] Schnars U, Jüptner W. Direct recording of holograms by a CCD target and numerical Reconstruction[J]. Appl. Opt., 1994, 33:179.

[4] Cheng-Shan Guo, Li Zhang, Zhen-Yu Rong, Hui-Tian Wang. Effect of the fill factor of CCD pixels on digital holograms: comment on the papers Frequency analysis of digital holography and Frequency analysis of digital holography with reconstruction by convolution[J]. Opt. Eng., 2003, 42(9):2768.

[5] Xu L, Miao J, Asundi A. Properties of digital holography based on in-line configuration[J]. Opt. Eng., 2000, 39 (12).

[6] Cuche E, Marquet P, Depeursinge C. Simultaneous amplitude-contrast and quantitative phase-contrast microscopy by numerical reconstruction of Fresnel offaxis holograms[J]. Appl. Opt., 1999,38(34):6994—7001.

[7] Schnars U, Kreis T M, Juptner W P O. Digital recording and numerical reconstruction of holograms: reduction of the spatial frequency spectrum[J]. Opt. Eng., 1996, 35:977—982.

[8] Goodman J W. Introduction to Fourier Optics[M]. McGraw-Hill Companies, Inc., New York, 1996.

[9] Kreis T M, Werner P O Juptner. Suppression of DC term in digital holography[J]. Opt. Eng., 1997,36(8):2357.

[10] Nazif Demoli, Jurica Mestrovic, Ivica Sovic. Subtraction digital holography[J]. Appl. Opt., 2003, 42(5):799.

[11] Liu C, Li Y,Cheng X,et al. Elimination of zero-order diffraction in digital holography[J]. Opt. Eng.,2002,41: 2434.

[12] Takaki Y, Kawai H, Ohzu H. Hybrid Holographic Microscopy Free of Conjugate and Zero-Order Images[J]. Appl. Opt.,1999, 38(23):4990.

[13] Zhang Y, Lu Q, Ge B. Elimination of zero-order diffraction in digital off-axis holography[J]. Optics Communication, 2004, 240(4):261.

[14] Adams M, Kreis T M, Juptner W P O. Particle size and position measurement with digital holography:, in Optical Inspection and Micromeasurements[J]. Proc. SPIE, 1997, 3098:234.

[15] Kreis T M, Adams M, Juptner W P O. Digital in-line holography in particle measurement[J]. Proc. of SPIE, 1999, 3744:54.

[16] Adams M, Kreis T, Juptner W. Particle Measurement with digital holography[J]. Proc. SPIE, 1999,3823.

[17] Shigeru Murata, Norifumi Yasuda. Potential of digital holography in particle measurement[J]. Optics and Laser Tech., 2000,32(7-8):567.

[18] Xu W, Jericho M H, Meinertzhagen I A, Kreuzer H J. Digital in-line holography of microspores[J]. Appl. Opt., 2002, 41(25):5367.

[19] Pan G, Meng H. Digital holography of particle fields: reconstruction by use of complex amplitude[J]. Appl. Opt., 2003, 42(5):827.

[20] Fournier C, Ducottet C, Fournel T. Digital in-line holography: influence of the reconstruction function on the axial profile of a reconstructed particle image[J]. Meas. Sci. Technol., 2004,15:686.

[21] Cuche E, Bevilacqua F, Depeursinge C. Digital holography for quantitative phase contrast imaging[J]. Optics letters, 1999,24(5):291.

[22] Pedrini G, Froning P H, Fessler H, Tiziani H J. Transient vibration measurement using multi-pulse digital holography[J]. Optics and Laser Technology,1997, 29(8):505.

[23] Mendoza Santiyo F, Pedrini G, Schedin S, Tiziani H J. 3D displacement measurements of vibrating objects with multi-pulse digital holography[J]. Meas. Sci. Technol., 1999,10:1305.

[24] Pedrini G, Schedin S, Tiziani H J. Lensless digital holographic interferometry for the measurement of large objects[J]. Opt. Comm., 1999,171:29.

[25] Schedin S, Pedrini G, Tiziani H J. Pulsed Digital Holography for Deformation Measurements on Biological Tissues[J]. Appl. Opt., 2000,39(16):2853.

[26] Schedin S, Pedrini G, Tiziani H J, Aggarwal A K, Gusev M E. Highly Sensitive Pulsed Digital Holography for Built-in Defect Analysis with a Laser Excitation[J]. Appl. Opt., 2001,40(1):100.

[27] Picart P, Leval J, Mounier D, Gougeon S. Time average digital holography[J]. Optics Letters, 2003, 28(20): 1900.